2022

Effect of boundary condition on shear behaviour of rock joint

Mairaj Soomro

Shivakumar Karekal

Buddhima Indraratna

EFFECT OF BOUNDARY CONDITION ON SHEAR BEHAVIOUR OF ROCK JOINT

Mairaj Soomro[1], Shivakumar Karekal[1] and Buddhima Indraratna[2]

ABSTRACT: The presence of inherent discontinuities within a rock mass poses significant influence on its shear strength-deformation characteristics. Therefore, it is important to study the rock joint performance within the laboratory for the safe and economical design of underground structures (such as mine roadways) in jointed rock mass, stability analysis of jointed rock slopes and foundation design on a fractured rock mass. To study the rock joint mechanics and principles governing its shear behaviour, this research is focused on the behaviour of natural rough rock joint within the laboratory under Constant Normal Load (CNL) and Constant Normal Stiffness (CNS) boundary condition using servo-controlled direct shear apparatus at the University of Wollongong, Australia. It was observed from the experimental results that the CNS testing procedure truly simulates the shearing mechanism of an actual field unlike CNL, and the shear strength evaluated rock joint is underestimated under the CNL boundary condition. Also, the shear strength envelope under CNS exhibits non-linearity in contrast with the bilinear strength envelope under CNL boundary condition.

INTRODUCTION

The mechanical behaviour of a jointed rock mass is governed by the discontinuities present within the rock mass, and these discontinuities can be in the form of joints, weak bedding planes, faults, etc. (ISRM, 1978). The heterogeneous nature of inherent discontinuities poses an inevitable threat to the stability of excavations, by significantly reducing the shear strength, derived within the rock mass; such as, mine roadways, tunnels, adit. Here, the term 'joint' is used to represent discontinuities. In other words, rock joints dominate the strength-deformation behaviour of a rock mass due to the spatial distribution of the asperities on the surface. Therefore, it is also important to correctly characterize the surface roughness of a rock joint. To evaluate the shear behaviour of rock joints within the laboratory, many researchers in the past have focused on the conventional direct shear test on rock joints where applied normal stress on the rock joint interface is kept constant throughout the shear test (Patton, 1966, Archambault et al., 1997, Ladanyi and Archambault, 1977, Bandis, 1983, Ghazvinian et al., 2010). This particular type of testing simulates the shear behaviour of planar joints, however, in the actual field, the rock joints are non-planar in nature and exhibit dilation, and this causes an inevitable increase in normal stress. Thus, the shearing process of a rock joint is no longer under Constant Normal Load (CNL); however, it is the stiffness of the surrounding rock mass that controls the shear behaviour, and this condition is shearing under Constant Normal Stiffness (CNS) boundary condition (Indraratna et al., 1998, Mirzaghorbanali et al., 2014, Indraratna et al., 2015, Thirukumaran and Indraratna, 2016) as shown in **Figure 1**.

The present study explains a non-contact procedure to characterize 3D surface roughness of a rock joint, and explains the effect of boundary conditions on the shear behaviour of the rock joint.

[1] *School of Civil, Mining, and Environmental Engineering, University of Wollongong. Email: skarekal@uow.edu.au, mhaas254@uowmail.edu.au*
[2] *Transport Research Centre, University of Technology Sydney. Email: buddhima.indraratna@uts.edu.au*

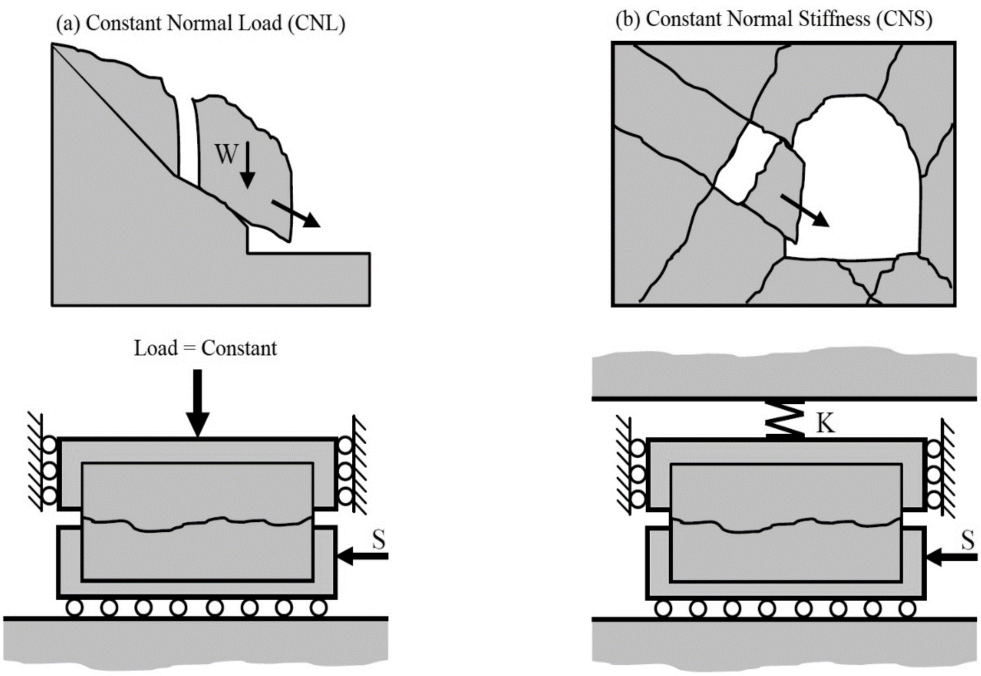

Figure 1: Boundary condition simulation within the direct shear test (a) CNL (b) CNS (Brady and Brown, 2005)

EXPERIMENTAL PROCEDURE

The shear strength-deformation behaviour was studied by conducting laboratory experiments on replicated natural rough rock joints under CNL and CNS boundary conditions using a servo-controlled large scale direct shear apparatus at the University of Wollongong, Australia. Researchers in the past have used different materials (such as, concrete), but Indraratna (1990) suggested the use of a mixture of hydro stone $(CaSO_4.2H_2O)$ and fine sand mixed with water to model soft sedimentary rocks. Also, the material is readily available, inexpensive and can be moulded into any shape when mixed with water. The long-term strength of the model material is independent of time after the chemical hydration process is complete.

A sandstone block was split into two halves to replicate a natural rough surface and then Silicon Rubber (SRT-30) was used to prepare rubber moulds to cast rock joint specimens for laboratory testing. The moulded specimens were cured in an oven with a controlled temperature of 38 - 40°C for two weeks. The average uniaxial compressive strength (σ_c), modulus of elasticity (E), and basic friction angle (ϕ_b) of the model material was 32.5 MPa, 10.1 GPa, and 30 degrees, respectively.

The surface roughness characterization of the test specimen was performed using a non-contact 3D scanner and digitiser (VIVID-910). Once scanned and digitized, the surface roughness was characterised and quantified using the joint roughness coefficient (JRC) model given by Tse and Cruden (1979). **Figure 2** shows a schematic of the 3D laser scanning system used in this study.

The 3D laser scanner was connected to a computer and was controlled and operated by the Polygon Editing Tool (PTE) software which operates, calibrates, registers, and merges multiple scans, and then scanned data was exported to quantify the Joint Roughness Coefficient (JRC). Multiple scans were taken to generate a complete 3D scan, and a fine scanning mode was utilized to enhance the accuracy of scanning with a 25mm of focal length lens at an approximately 1m working distance maintained for all scans performed, as suggested by Indraratna et al. (2021) and Soomro et al. (2022). The potential shear direction is well-defined in most cases; therefore, the roughness of a rock joint is evaluated from cross-sectional profiles taken parallel to the potential shear direction as suggested by ISRM (1978). To obtain the rock joint profiles along the defined shear direction, the 3D scan of each rock joint specimen surface was digitized at an equal interval of 5 mm, and 23 cross-sectional profiles were taken, and the JRC of each profile was determined and the average was taken as a representative JRC as shown in **Figure 3**.

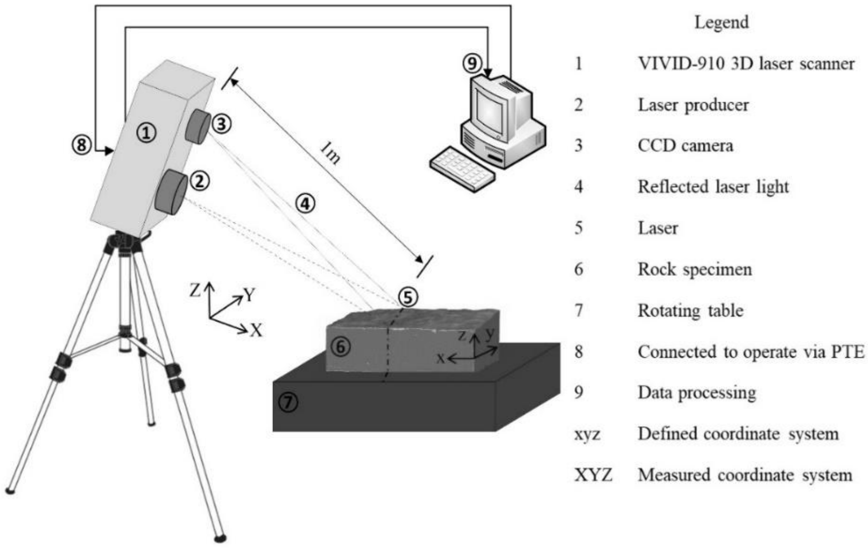

Figure 2: Schematic of 3D laser scanning system

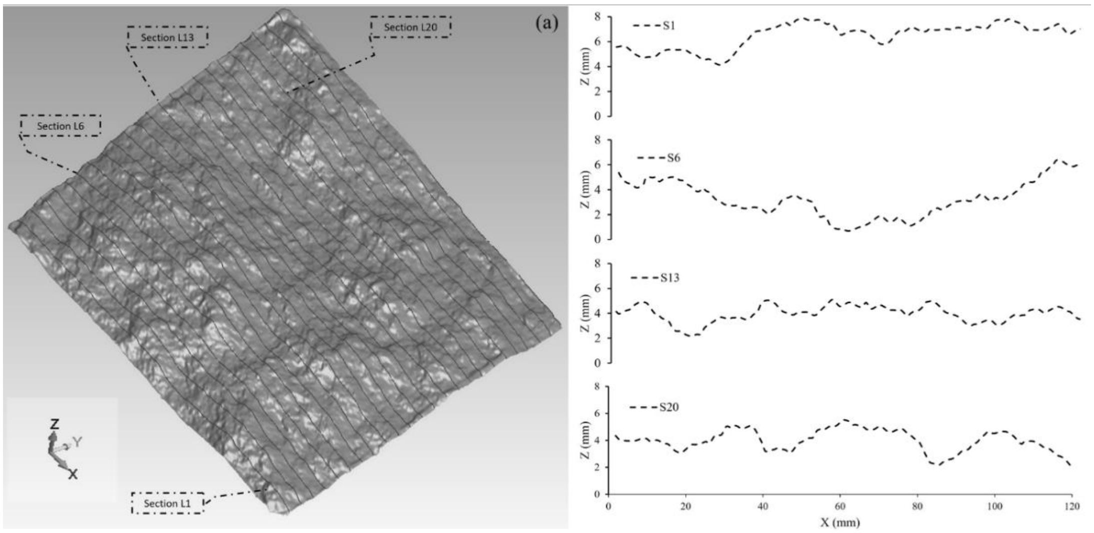

Figure 3: Digitization of rock joint (surface) specimen

The JRC quantification was carried out as proposed by Barton and Choubey (1977) and recommended by ISRM (1978). This procedure involved visual matching of each section with 10 standard roughness profiles, however, Beer et al. (2002) suggested that visual matching of each profile could be subjective, and many researchers presented different methods to quantify the roughness parameter (Grasselli et al., 2002, Yang et al., 2001, Indraratna and Haque, 2000), however, the roughness parameter Z_2 given by Tse and Cruden (1979) has the highest R^2 value and is written as:

$$JRC = 32.2 + 32.47 \log Z_2 \tag{1}$$

where Z_2 is the root mean square of the first derivative of the roughness profile, and it can be expressed in the following discrete form:

$$Z_2 = \left[\frac{1}{L_n}\sum_{i=1}^{n-1}\frac{(y_{i+1}-y_i)^2}{(x_{i+1}-x_i)}\right]^{1/2} \tag{2}$$

where (x_i, y_i) and (x_{i+1}, y_{i+1}) represent the adjacent coordinates of the roughness profile separated by the sample interval of Δx and Δy respectively, n is the number of measurement points, and L_n is the nominal length of the profile as shown in the **Figure 4.**

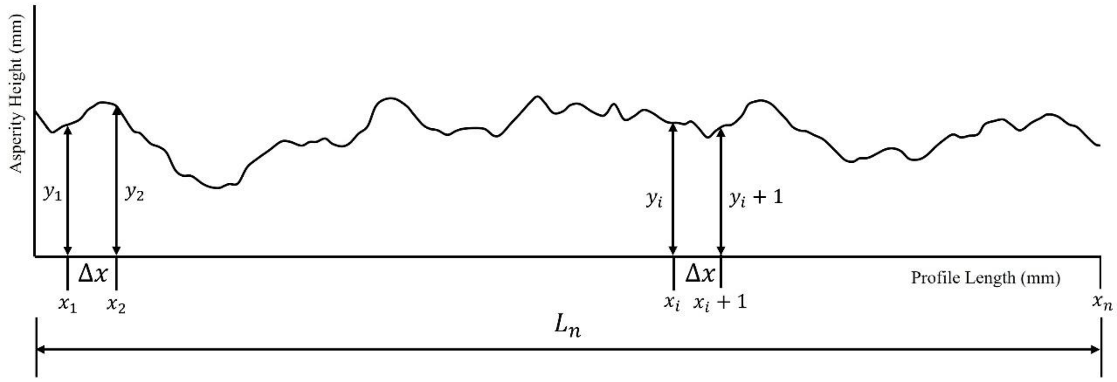

Figure 4: Definition of roughness parameter (Z_2)

The basic statistical analysis of JRC of a rock joint specimen is given in **Table 1**, and the mean value is selected as the JRC of the test specimen.

Table 1: Statistical analysis of JRC values of each type of specimen

Direct Shear Test Specimen	Joint Roughness Coefficient (JRC)			
	Mean	Minimum	Maximum	Standard Deviation
	11.7	11.54	11.86	0.158

In this study, both types of testing was performed to observe the shear behaviour of rock joints under CNL and CNS boundary conditions. To conduct the testing, a large-scale servo-controlled direct shear testing machine, designed at the University of Wollongong (UOW) Australia, and built by CMA Engineering, Illawarra, was used to perform the direct shear experiments under CNL and CNS condition. The equipment consisted of four main parts; controller unit, mechanical section, hydraulic section, and cooler section as shown in **Figure 5**. The shear box consists of upper and lower parts; the upper part moves vertically and the lower part moves horizontally, and two actuators are used to apply the load in both vertical and horizontal directions.

The servo-controlled hydraulic system is composed of an electro-hydraulic vertical actuator with a 50kN load capacity, 80mm vertical stroke length with electro-hydraulic servo-valve for closed loop control of vertical load and vertical displacement, and an electro-hydraulic horizontal actuator with a 50kN load capacity, and ±90mm horizontal stroke length and an electro-hydraulic servo valve for closed loop control of shear load and shear displacement. Shear and normal loads are measured by load cells, and shear and normal displacements are measured by using the Balluff's Magnetostrictive Sensors for higher accuracy and reliability in position and speed measurements over long stroke lengths with a linear deviation of ±30µm.

Figure 6 shows testing procedure adopted to perform direct shear tests, and **Table 2** shows input parameters used for testing.

Furthermore, to calculate the shear stress (τ) and normal stress (σ_n) at any shear displacement (δ_h), the following equations were used:

$$\tau = \frac{S}{B(L - \delta_h)} \tag{3}$$

$$\sigma_n = \frac{N}{B(L - \delta_h)} \tag{4}$$

where S is the shear load and N is the normal load any shear displacement (δ_h), L is the length of the specimen, and B is the width of the specimen.

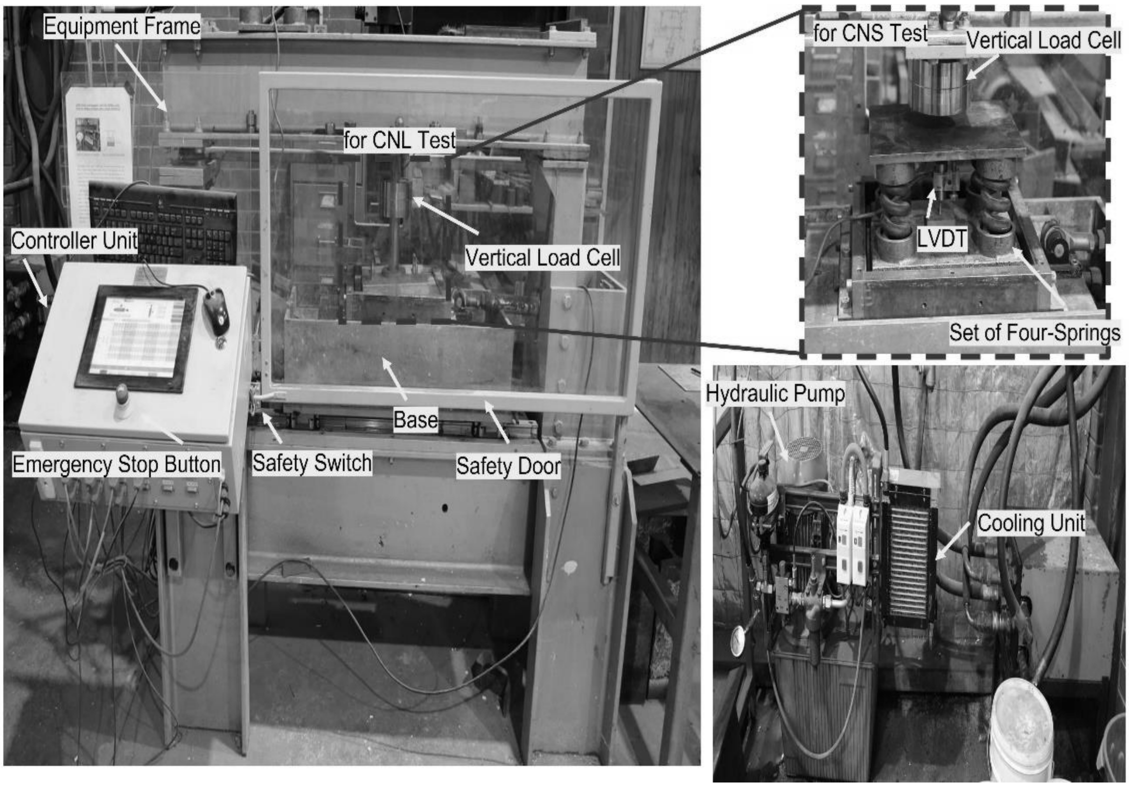

Figure 5: UOW servo-controlled direct shear equipment

Figure 6: Direct Shear Testing Procedure

Table 2: Input parameters

Series	Test Type	JRC	Initial Normal Stress (σ_{no}, MPa)	Boundary Condition	Stiffness (K_n/mm)	Shear Rate (mm/min)
DST-I	Static	11.7	0.25, 0.5, 1.0	CNL and CNS	8	0.1

RESULTS AND DISCUSSION

The direct shear experiments were performed under monotonic loading conditions to study the shear behaviour of rock joints under CNL and CNS boundary conditions. Initially, the direct shear tests were performed under CNL, and then CNS to observe the effect of boundary conditions. The tests were performed on a rock joint specimen (casted using a model material) with a joint roughness coefficient (JRC) of 11.7 at an initial normal stress (σ_{no}) of 0.25 MPa, 0.50 MPa, and 1.0 MPa with a shear rate of 0.1 mm/min under zero constant normal stiffness (CNL) and 8.0 kN/mm of constant normal stiffness (CNS) boundary condition. The shear behaviour of the rock joint specimen under CNL and CNS is plotted in **Figure 7**. Shear and normal loads were determined by using Eq. (3) and Eq. (4) respectively, as it incorporates an area correction for accurate determination of shear and normal stresses. As anticipated, the peak shear stress of the rock joint specimen under CNL is underestimated because the specimen is allowed to dilate freely, however, the peak shear stress tends to increase with an increase in horizontal displacement under CNS due to a change in normal stress. Under CNL, the peak shear stress is reached and then it is stabilized throughout the remainder of the test, however, under CNS, the continuous effect of a change in normal stress and restricted dilation is clearly observed with an increase in shear stress along the horizontal displacement. It is interesting to see that, under CNL, the peak shear stress is almost reaching to the applied normal stress (σ_{no}), and the constant shear stress after reaching the peak is also indicating the free dilation as shown in the horizontal-vertical displacement plot if **Figure 7.** Strain hardening behaviour was observed under CNL, however, the rock joint specimen is exhibiting strain softening behaviour under CNS boundary conditions. It is also interesting to see that the shear strength envelope under the CNL boundary conditions is showing bilinear behaviour, however, the shear strength envelope under CNS boundary conditions is showing highly non-linear behaviour as shown in **Figure 8**.

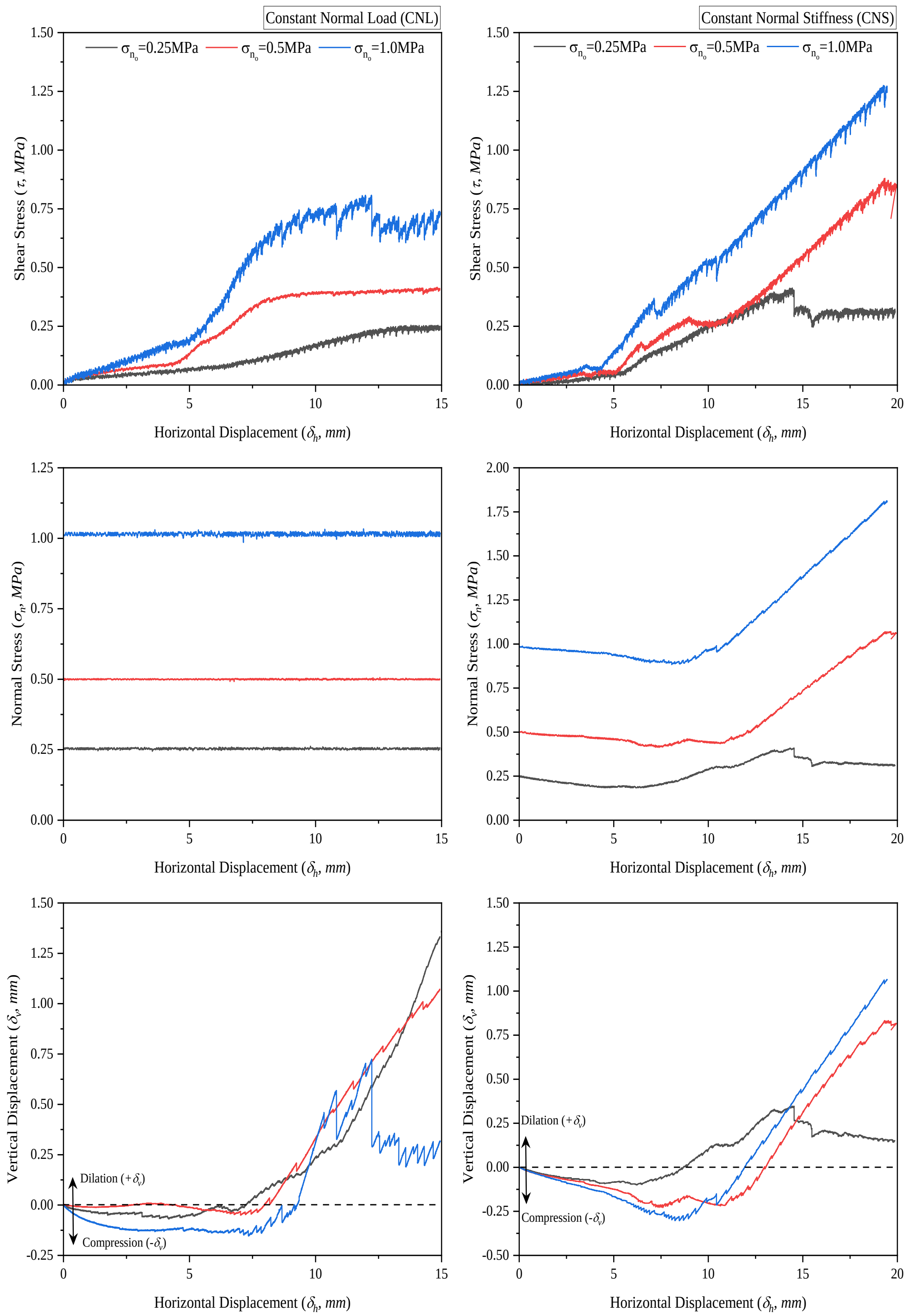

Figure 7: Shear behaviour of rock joint under CNL and CNS boundary condition

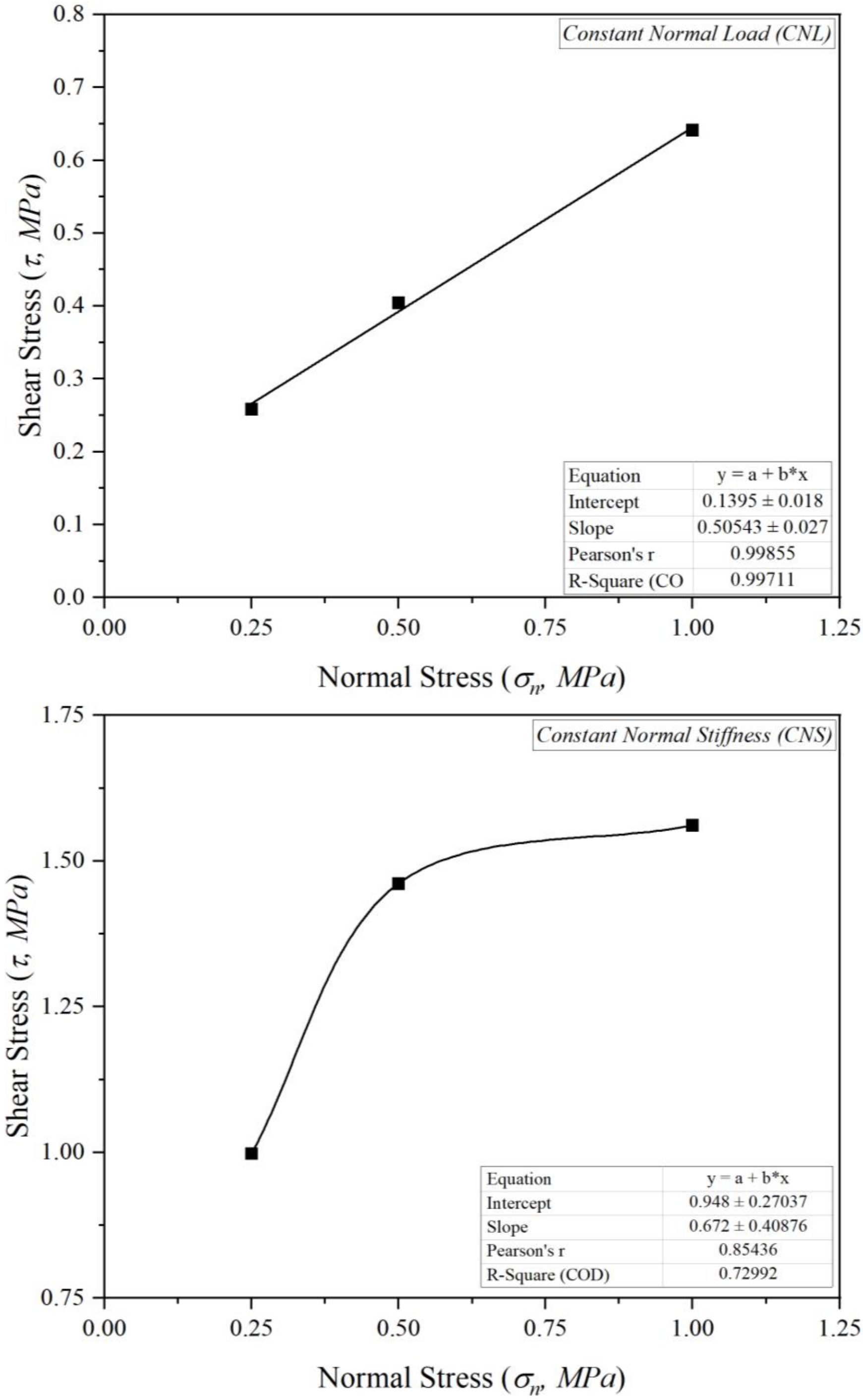

Figure 8: Strength envelope of rock joint under CNL and CNS boundary conditio

CONCLUSIONS

Shear behaviour of a rock joint with a JRC of 11.7 was studied under CNL and CNS boundary conditions by using servo-controlled direct shear equipment. Under CNL, the normal stress remains constant, however, under CNS, normal stress changes with horizontal displacement and the variation in normal stress follows the surface roughness profile of asperities. Shear strength of the rock joint is underestimated under CNL due to the reduced contact of asperities because of free dilation, however, shear strength under CNS is more than CNL because of increased asperities contact due to a variation in normal stress with horizontal displacement. The strength envelope of rock joint under CNL is observed to be bilinear, however, it is non-linear under CNS boundary conditions.

ACKNOWLEDGMENTS

The first author wishes to acknowledge the joint Ph.D. scholarship provided by Higher Education Commission (HEC) Pakistan and University of Wollongong, Australia, along with the study leave granted by Mehran University of Engineering and Technology, Jamshoro, Pakistan. The authors wish to acknowledge the contributions of Mr. Richard Berndt, Mr. Jordan Wallace, Mr. Ritchie Mclean, Mr. Travis Marshall (Senior Technical Officers, University of Wollongong, Australia) during laboratory testing.

REFERENCES

ARCHAMBAULT, G., GENTIER, S., RISS, J. and FLAMAND, R. 1997. The evolution of void spaces (permeability) in relation with rock joint shear behavior. *International Journal of Rock Mechanics and Mining Sciences,* 34**,** 14.e1-14.e15.

BANDIS, S. L., A; BARTON, N 1983. Fundamentals of rock joint deformation. *International Journal of Rock Mechanics and Mining Sciences and Geomechanics*.

BARTON, N. and CHOUBEY, V. 1977. The shear strength of rock joints in theory and practice. *Rock Mechanics Felsmechanik Mcanique des Roches,* 10**,** 1-54.

BEER, A. J., STEAD, D. and COGGAN, J. S. 2002. Technical Note Estimation of the Joint Roughness Coefficient (JRC) by Visual Comparison. *Rock Mechanics and Rock Engineering,* 35**,** 65-74.

BRADY, B. H. and BROWN, E. T. 2005. *Rock Mechanics: for Underground Mining*, Springer science and business media.

GHAZVINIAN, A., TAGHICHIAN, A., HASHEMI, M. and MAR'ASHI, S. 2010. The shear behavior of bedding planes of weakness between two different rock types with high strength difference. *Rock Mechanics and Rock Engineering,* 43**,** 69-87.

GRASSELLI, G., WIRTH, J. and EGGER, P. 2002. Quantitative three-dimensional description of a rough surface and parameter evolution with shearing. *International Journal of Rock Mechanics and Mining Sciences,* 39**,** 789-800.

INDRARATNA, B. 1990. Development and applications of a synthetic material to simulate soft sedimentary rocks. *Geotechnique,* 40**,** 189-200.

INDRARATNA, B. and HAQUE, A. 2000. *Shear behaviour of rock joints*, CRC Press.

INDRARATNA, B., HAQUE, A. and AZIZ, N. 1998. Laboratory modelling of shear behaviour of soft joints under constant normal stiffness conditions. *Geotechnical and Geological Engineering,* 16**,** 17-44.

INDRARATNA, B., SOOMRO, M. H. A. A. and RUJIKIATKAMJORN, C. 2021. Semi-empirical analytical modelling of equivalent dynamic shear strength (EDSS) of rock joint. *Transportation Geotechnics,* 29**,** 100569.

INDRARATNA, B., THIRUKUMARAN, S., BROWN, E. and ZHU, S.-P. 2015. Modelling the shear behaviour of rock joints with asperity damage under constant normal stiffness. *Rock Mechanics and Rock Engineering,* 48**,** 179-195.

ISRM 1978. Suggested methods for the quantitative description of discontinuities in rock masses. *International Journal of Rock Mechanics and Mining Sciences and Geomechanics,* 15**,** 319-368.

LADANYI, B. and ARCHAMBAULT, G. Shear strength and deformability of filled indented joints. Proc International Symposium on the Geotechnics of Structurally Complex Formations. Capri, 1977. 317-326.

MIRZAGHORBANALI, A., NEMCIK, J. and AZIZ, N. 2014. Effects of shear rate on cyclic loading shear behaviour of rock joints under constant normal stiffness conditions. *Rock mechanics and rock engineering,* 47**,** 1931-1938.

PATTON, F. D. Multiple modes of shear failure in rock. 1st ISRM Congress, 1966. International Society for Rock Mechanics.

SOOMRO, M. H. A. A., INDRARATNA, B. and KAREKAL, S. 2022. Critical shear strain and sliding potential of rock joint under cyclic loading. *Transportation Geotechnics,* 32**,** 100708.

THIRUKUMARAN, S. and INDRARATNA, B. 2016. A review of shear strength models for rock joints subjected to constant normal stiffness. *Journal of Rock Mechanics and Geotechnical Engineering,* 8**,** 405-414.

TSE, R. and CRUDEN, D. M. 1979. Estimating joint roughness coefficients. *International Journal of Rock Mechanics and Mining Sciences and Geomechanics Abstracts,* 16**,** 303-307.

YANG, Z., LO, S. and DI, C. 2001. Reassessing the joint roughness coefficient (JRC) estimation using Z 2. *Rock mechanics and rock engineering,* 34**,** 243-251.